


Oscillatory Instabilities in Frictional Granular Matter

Joyjit Chattoraj,¹ Oleg Gendelman,² Massimo Pica Ciamarra,^{1,3,*} and Itamar Procaccia⁴
¹*School of Physical and Mathematical Sciences, Nanyang Technological University, 637371 Singapore*
²*Faculty of Mechanical Engineering, Technion, Haifa 32000, Israel*
³*CNR-SPIN, Dipartimento di Scienze Fisiche, Università di Napoli Federico II, I-80126, Napoli, Italy*
⁴*Department of Chemical Physics, Weizmann Institute of Science, Rehovot 76100, Israel*

 (Received 7 January 2019; published 30 August 2019)

Frictional granular matter is shown to be fundamentally different in its plastic responses to external strains from generic glasses and amorphous solids without friction. While regular glasses exhibit plastic instabilities due to the vanishing of a real eigenvalue of the Hessian matrix, frictional granular materials can exhibit a previously unnoticed additional mechanism for instabilities, i.e., the appearance of a pair of complex eigenvalues leading to oscillatory exponential growth of perturbations that are tamed by dynamical nonlinearities. This fundamental difference appears crucial for the understanding of plasticity and failure in frictional granular materials. The possible relevance to earthquake physics is discussed.

DOI: [10.1103/PhysRevLett.123.098003](https://doi.org/10.1103/PhysRevLett.123.098003)

It is often stressed that the mechanical properties of frictional granular matter and of glassy amorphous solids share many similarities [1–5]. However, the presence of friction implies that the effective forces in frictional solids are not derivable from a Hamiltonian. While Hamiltonian models might in some cases mimic non-Hamiltonian ones [6,7], here we show that the absence of a Hamiltonian implies the existence of previously unreported oscillatory instabilities in frictional granular matter that cannot exist in Hamiltonian systems. These oscillatory instabilities furnish a micromechanical mechanism for a giant amplification of small perturbations that can lead eventually to major events of mechanical failure. We will demonstrate this physics in the context of amorphous assemblies of frictional disks, but will make the point that the mechanism discussed here is generic for systems with friction.

To motivate the new ideas recall that the understanding of plastic instabilities, shear banding, and mechanical failure in athermal amorphous solids with an underlying Hamiltonian description has progressed significantly in the last 20 years. Beginning with the seminal papers of Malandro and Lacks [8,9], it became clear that an object that controls the mechanical responses of athermal glasses is the Hessian matrix. In an athermal ($T = 0$) system of N particles at positions $(\mathbf{r}_1, \mathbf{r}_2, \dots, \mathbf{r}_N)$ we define the Hamiltonian $U(\mathbf{r}_1, \mathbf{r}_2, \dots, \mathbf{r}_N)$. The Hessian matrix is

$$H_{ij}^{\alpha\beta} \equiv \frac{\partial^2 U(\mathbf{r}_1, \mathbf{r}_2, \dots, \mathbf{r}_N)}{\partial r_i^\alpha \partial r_j^\beta} = -\frac{\partial F_i^\alpha}{\partial r_j^\beta}. \quad (1)$$

Here \mathbf{F}_i is the total force on the i th particle, and in systems with binary interactions we can write $\mathbf{F}_i \equiv \sum_j \mathbf{F}_{ij}$ with the sum running on all the particles j interacting with particle i .

Being real and symmetric, the Hessian matrix has real eigenvalues that are all positive as long as the material is mechanically stable. Under strain, the system may display a saddle node bifurcation in which an eigenvalue goes to zero, accompanied by a localization of an eigenfunction, signaling a plastic instability that is accompanied by a drop in stress and energy [10]. A significant amount of work was dedicated to understanding the density of states of the Hessian matrix, which differs in amorphous solids from the classical Debye density of purely elastic materials [3,11,12]. The well-known “Boson peak” was explained by the prevalence of “plastic modes” that can go unstable and do not exist in pure elastic systems. The system size dependence of the eigenvalues of the Hessian [11], their role in determining the mechanical characteristics like the elastic moduli [13], the failure of nonlinear elasticity in such materials [13–15], and the relevance to shear banding and mechanical failure [16–18] all underline the importance of this approach to the theory of amorphous solids.

Alas, this useful approach appears to be irretrievably lost when we consider the available models for *frictional* granular media with both normal and tangential forces at every contact of two granules. The reason is twofold. First, the tangential forces $\mathbf{F}_{ij}^{(t)}$ (see below for details) are not analytic because of the Coulomb constraint, $|\mathbf{F}_{ij}^{(t)}| \leq \mu |\mathbf{F}_{ij}^{(n)}|$, bounding the magnitude of the tangential force by the normal force $\mathbf{F}_{ij}^{(n)}$ multiplied by μ , which is the friction coefficient. Second, and most important, forces in granular systems are history dependent and hence not derivable from a Hamiltonian. The history dependence is a key feature of the granular interaction, retained by all interaction models, such as the popular Hertz-Mindlin one [19], where interparticle forces are derived by coarse graining the highly

complex microscopic mechanics of compressed granules. As the resulting model forces cannot be derived from a Hamiltonian function, they are not energy conserving. We stress that this occurs also in the absence of viscous damping and before the Coulomb limit is reached.

To describe the failure of a granular system as a dynamical instability, we follow a two-step approach. The first (maybe trivial looking) step that we propose here is to smooth out the approach to the Coulomb limit to allow differentiating the tangential force [see Eq. (7) below]. In the second step, we consider frictional disks for which the coordinates now include the positions \mathbf{r}_i of the centers of mass and the angles θ_i of each disk. The Newton equations of motion are written as

$$\begin{aligned} m_i \frac{d^2 \mathbf{r}_i}{dt^2} &= \mathbf{F}_i(\mathbf{q}_1, \mathbf{q}_2, \dots, \mathbf{q}_N), \\ I_i \frac{d^2 \theta_i}{dt^2} &= \mathbf{T}_i(\mathbf{q}_1, \mathbf{q}_2, \dots, \mathbf{q}_N), \end{aligned} \quad (2)$$

where $\mathbf{q}_i \equiv \{\mathbf{r}_i, \theta_i\} \equiv \{r_i^x, r_i^y, \theta_i\}$ and m_i, I_i are masses and moment of inertia. It is important to stress that the forces in Eq. (2) depend only on the generalized coordinates \mathbf{q}_j ; i.e., first derivatives do not appear. The stability of the system is then determined by an operator obtained from the derivatives of $\tilde{\mathbf{F}}_i = (\mathbf{F}_i, \mathbf{T}_i)$ (see Supplemental Material for details [20]). In other words,

$$\mathbf{J}_{ij} \equiv -\frac{\partial \tilde{\mathbf{F}}_i}{\partial \mathbf{q}_j}. \quad (3)$$

The analogy between the operator \mathbf{J} and the Hessian matrix is apparent. However, there is a huge difference for which the consequences are explored below. \mathbf{J} is not a symmetric operator. Accordingly, it can have real eigenvalues as the Hessian, but it can also display a number of eigenvalues as complex conjugate pairs. When a pair of complex eigenvalues, $\lambda_{1,2} = \lambda_r \pm i\lambda_i$, gets born, a novel instability mechanism develops. Indeed, these eigenvalues correspond to *four* solutions $e^{i\omega t}$ to the linearized equation of motion, with

$$i\omega_{1,2} = \omega_i \pm i\omega_r, \quad i\omega_{3,4} = -\omega_i \pm i\omega_r, \quad (4)$$

with $\omega_r \pm i\omega_i = \sqrt{\lambda_r \pm i\lambda_i}$. The first pair in (4) induces an oscillatory motion with an exponential growth of any deviation $\mathbf{q}(0)$ from a state of mechanical equilibrium,

$$\mathbf{q}(t) = \mathbf{q}(0)e^{\omega_i t} \sin(\omega_r t). \quad (5)$$

The second pair represents an exponentially decaying oscillatory solution. Note that this bifurcation is not a regular Hopf bifurcation. It needs at least four degrees of freedom (four first-order or two second-order differential equations). This is a somewhat unusual bifurcation that is

due to the symmetry of the equations of motion that lack first derivatives. We also comment again that such a bifurcation is impossible in frictionless amorphous solids with a microscopic Hamiltonian.

To validate this theoretical scenario and explore its consequences, we focus on a binary assembly of N frictional disks of mass m in a box of size L^2 , half of which with radius $\sigma_1 = 0.5$ and the other half with $\sigma_2 = 0.7$. Under external stress, they interact with binary interactions; the normal force is determined by the overlap $\delta_{ij} \equiv \sigma_i + \sigma_j - r_{ij}$, where $\mathbf{r}_{ij} \equiv \mathbf{r}_i - \mathbf{r}_j$. The normal force is Hertzian,

$$\mathbf{F}_{ij}^{(n)} = k_n \delta_{ij}^{3/2} \hat{\mathbf{r}}_{ij}, \quad \hat{\mathbf{r}}_{ij} \equiv \mathbf{r}_{ij}/r_{ij}. \quad (6)$$

The tangential force is determined by the tangential displacement \mathbf{t}_{ij} , the integral of the velocity at the contact point over the duration of the contact, rotated so as to enforce $\mathbf{t}_{ij} \hat{\mathbf{r}}_{ij} = 0$ at all times. This is quite standard [21]. We deviate from the standard in the definition of the tangential force, which we assume to be

$$\begin{aligned} \mathbf{F}_{ij}^{(t)} &= -k_t \delta_{ij}^{1/2} \left[1 + \frac{t_{ij}}{t_{ij}^*} - \left(\frac{t_{ij}}{t_{ij}^*} \right)^2 \right] t_{ij} \hat{\mathbf{t}}_{ij}, \\ t_{ij}^* &\equiv \mu \frac{k_n}{k_t} \delta_{ij}, \end{aligned} \quad (7)$$

with $k_t = 2k_n/7$ [21]. The derivative of the force with respect to t_{ij} vanishes smoothly at $t_{ij} = t_{ij}^*$, and the Coulomb law is fulfilled. In the following, we use as units of mass, length, and time $m, 2\sigma_1$, and $\sqrt{m(2\sigma_1)^{-1/2}k_n^{-1}}$, respectively.

We demonstrate the new type of instability considering a system with $N = 500$. We prepare a mechanically equilibrated amorphous system with packing fraction 0.86 and friction coefficient $\mu = 0.5$ in a periodic two-dimensional box. Upon straining we can let the system evolve, solving according to Eq. (2), with the forces given by Eqs. (6) and (7), and with the addition of a damping force proportional to the velocities of the particles with a coefficient of proportionality $m\eta$. When $\eta = 0$, we are solving a Newtonian dynamics, which is the one for which we have theoretical predictions. When the damping timescale η^{-1} is very small, e.g., of the order of the time that sound waves need to travel one particle diameter [22], the dynamics is overdamped. In this limit, even in the presence of complex eigenvalues, the oscillatory instability is suppressed, as accelerations can be neglected and the equations of motion become of first order. In the following, we use these two limiting dynamics to validate our theoretical results and then discuss the role of damping. The numerical solution of the equation of motion is carried out with LAMMPS [23] while setting the integration time step $10^{-5} \sqrt{m^{-1}(2\sigma_1)^{1/2}k_n}$.

An athermal quasistatic shear protocol is now devised using the Lees-Edwards boundary conditions as follows:

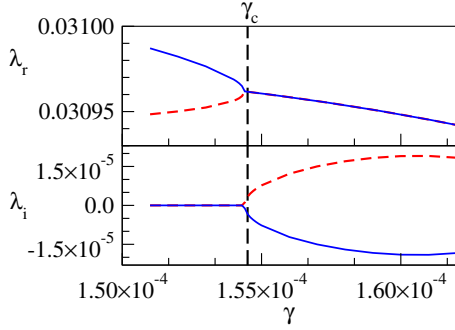


FIG. 1. Upon increasing the strain γ two modes with real eigenvalues λ coalesce at γ_c (dashed vertical lines), and a pair of complex conjugate modes gets born. The upper and the lower halves show the evolution of the real and imaginary components of these modes.

Starting from the initial stable configuration, the system is sheared along the horizontal direction (x) by the amount $\delta\gamma$, varied in the range 10^{-4} – 10^{-8} depending on the precision needed for the identification of the instability. Thus, each particle experiences an affine shift along x depending on their vertical coordinates r_i^y , i.e., $\delta r_i^x = \delta\gamma r_i^y$. Next, we run the overdamped dynamics to bring the system back to mechanical equilibrium where the net force on each particle is less than 5×10^{-12} . After every such step, we diagonalize the matrix \mathbf{J} to find its eigenvalues. At some value of γ , we find for the first time the birth of a conjugate pair of complex eigenvalues, as seen in Fig. 1. If we continue to increase the strain using the same protocol, we see the emergence of other complex pairs at the expense of real eigenvalues.

To explore how the system responds to the bifurcation and validate our theoretical predictions, we then run a Newtonian dynamics. As an example, we do it here starting from a configuration with two complex conjugate eigenpairs. The dominant eigenpair, which is the one with the largest growth rate ω_i , has $\omega_r \simeq 0.17$, $\omega_i \simeq 5.4 \times 10^{-5}$.

During the Newtonian dynamics, we evaluate the operator \mathbf{J} and its eigenvalues. We find that all the eigenvalues remain invariant for a long stretch of time, as illustrated in Fig. 2(a), until a major instability takes place. The system is expected to follow the prediction of our linear stability analysis as long as the eigenvalues remain constant. Insight into the expected particle motion is obtained considering that real matrices admit a real eigendecomposition of the kind $\mathbf{J} = \mathbf{C}\mathbf{D}\mathbf{C}^{-1}$ with \mathbf{C} , the square matrix whose columns are the eigenvectors of \mathbf{J} . If \mathbf{J} is symmetric, then \mathbf{D} is the diagonal matrix containing the eigenvalues. If \mathbf{J} is not symmetric, then \mathbf{D} is block diagonal. The blocks are 1×1 blocks containing the real eigenvalues, or rotation-scaling blocks $|\lambda|\mathbf{R}(\theta)$ with \mathbf{R} 2×2 rotation matrix, one block for each complex eigenvalue pair $|\lambda|e^{\pm i\theta}$. This clarifies that the complex eigenvalues, i.e., the rotation-scaling blocks, induce a spiral motion. The emergence of this spiral motion

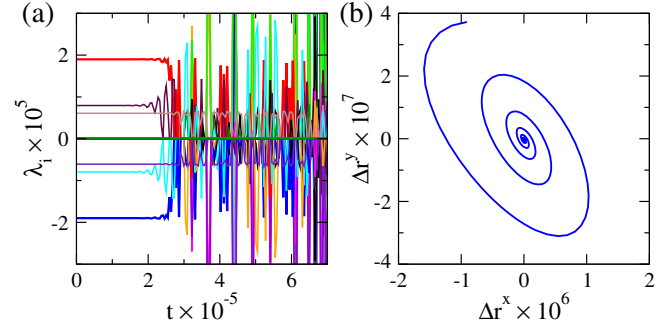


FIG. 2. (a) Time dependence of the imaginary component of all 1500 eigenvalues of the system, during a Newtonian simulation. (b) Typical spiral trajectory of a particle in the linear response regime.

is illustrated in the Supplemental Material video [20]. The spiral trajectory of a randomly selected particle is shown in Fig. 2(b).

Next we consider the mean-square displacement $M(t)$ as a function of time. Denoting $\Delta r_i^x(t) \equiv r_i^x(t) - r_i^x(t=0)$, etc., we define

$$M(t) \equiv \frac{1}{N} \sum_i^N ([\Delta r_i^x(t)]^2 + [\Delta r_i^y(t)]^2 + \sigma_i^2 [\Delta \theta_i(t)]^2), \quad (8)$$

which according to Eq. (5) should behave as $M(t) \propto e^{2\omega_i t} \sin^2(\omega_r t)$. Indeed, we see in Fig. 3 that $M(t)$ shoots up in time about 8 orders of magnitude with exponential rate while following the oscillatory motion. The growth rate and the oscillatory frequencies match precisely the linear

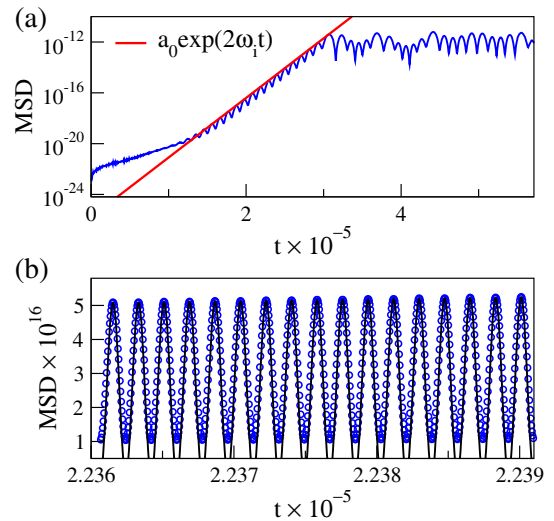


FIG. 3. (a) The numerically computed mean-square displacement as a function of time. The red line is the predicted exponential growth from the linear instability $a_0 e^{2\omega_i t}$, with a_0 being fitted. (b) An enlargement of the growth of the mean-square displacement. The black line is the exponential oscillatory instability prediction, $a_0 e^{2\omega_i t} [\sin(\omega_r t + \psi)]^2$, with ψ fitted.

instability prediction. We have also checked that the rotational contribution to $M(t)$ behaves as expected [24]. We remark that, due to numerical noise as well as to the overdamped dynamics used to prepare the initial configuration, both the unstable mode and few stable modes contribute to the MSD. Indeed, we observe in Fig. 3(a) that the instability dominates the response after a short transient, the first modes contributing to the mean-square displacement being the high frequency stable ones. At longer times these stable modes simply contribute a small constant to the mean square displacement (MSD). This constant is the small value the MSD of Fig. 3(b) periodically reaches.

Finally, we focus on the virial component of the shear stress $\sigma_{xy} = -(1/L^2) \sum_{i \neq j}^N r_{ij}^x F_{ij}^y$. During the development of the instability, the stress change is predicted to evolve as $\sigma_{xy}(t) - \sigma_{xy}(0) \propto e^{\omega_r t} \sin(\omega_r t + \psi)$. Figure 4(a) shows that the stress follows the predicted linear instability with its exponential growth and oscillations until the perturbation self-amplifies enough to induce a plastic instability in which the system undergoes a microearthquake.

Taken together, Figs. 2(a), 3(a), and 4(a) indicate that the predictability of the evolution under the effect of the oscillatory exponential instability terminates at a time $t \approx 3 \times 10^5$. Around that time, the perturbation amplified enough for the system to switch on a nonlinear response characterized by the coexistence of a number of unstable modes, saturating the mean-square displacement and causing large stress fluctuations. At longer times, these fluctuations cause a series of failure events, leading to a reduction of shear stress [24].

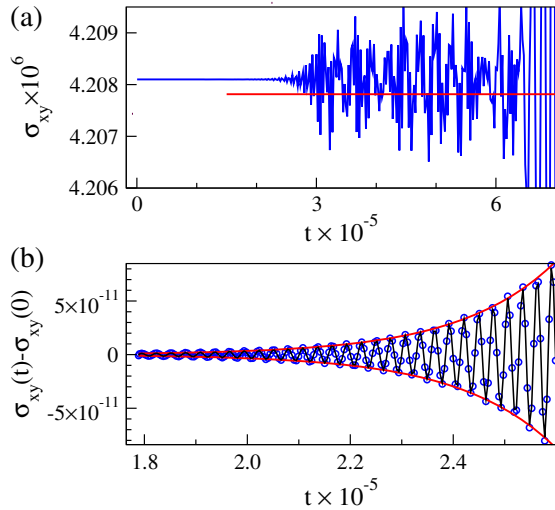


FIG. 4. (a) Evolution of shear stress (virial contribution) σ_{xy} during Newtonian dynamics. The instability results in a drop in the average stress. The red line denotes the average stress after the linear response regime. (b) Enlargement of the stress change during the development of the instability. The black line is the theoretical prediction $\Delta\sigma e^{\omega_r t} \sin(\omega_r t + \psi)$, with a fitted ψ and $\Delta\sigma$; the red lines mark the envelope $\pm\Delta\sigma e^{\omega_r t}$.

The oscillatory instability was demonstrated neglecting any damping. The role of damping is the introduction of a typical timescale η^{-1} , which competes with the growth rate of the instabilities ω_i . We find that, only if the damping timescale is smaller than ω_i^{-1} , the instability is suppressed [24]. Importantly, we show in Supplemental Material Fig. S1 [20] that the instability is observed in the presence of dissipation in the interparticle interaction force, with standard values of the dissipation parameters, explicitly demonstrating that our findings are relevant to granular systems.

At this point, it is important to stress that the existence of the oscillatory instability is not limited to the particular choice of forces [Eqs. (6) and (7)]. Any reasonable coarse-grained theory of tangential forces must take into account the fact that compressed granules will create a larger area of contact. Accordingly, it is expected that the tangential force will be a function not only of the θ_i coordinates but also of the positional coordinates r_i . Consequently, in general, the forces would not be derivable from a Hamiltonian, and the corresponding operator \mathbf{J} would not be symmetric. There is therefore a generic possibility to find complex eigenpairs in this operator in any reasonable coarse-grained theory of frictional matter. We have checked, for instance, that the Harmonic model, rather than the Hertzian one discussed in this Letter, also leads to the reported instabilities. There is also the possibility that these oscillatory instabilities are not experimentally observed: this would imply that the coarse-grained models the whole granular community has been using in the last ~ 50 years lead to unphysical results and should be revised.

We would like to finally speculate that our results could be relevant to the physics of earthquakes. A striking observation in earthquake physics is known as “remote triggering” [25–27]: an earthquake could trigger a subsequent earthquake on a different fault, even if located far away. It is clear that faults can “communicate” via seismic waves propagating through the Earth’s crust. However, distant faults can only communicate via long wavelength seismic waves, as short wavelengths are quickly damped as they propagate. Since long wavelengths act as small perturbations, as they have a small frequency and hence a small energy density, it is not clear how they could be able to induce the failure of a fault. The most popular approach to rationalize this observation within the geophysical community, the acoustic fluidization [28,29] mechanism, suggests that long wavelengths impacting on a fault trigger short wavelengths within the fault, and that these act by reducing the confining pressure and promoting failure. However, a detailed micromechanical investigation of this process is lacking. Our results might be relevant in this context as they provide a clear mechanism for the self-amplification of small perturbations. We of course do not propose that the system studied above of frictional disks includes all the rich physics of the Earth and its faults, but it

is quite worthwhile to study this mechanism also in the context of fault dynamics and in other contexts of frictional granular matter and, more generally, in systems lacking a Hamiltonian description [30].

This work has been supported in part by the ISF-Singapore exchange program and by the US-Israel Binational Science Foundation. We thank Jacques Zylberg and Yoav Pollack for useful discussions and exchanges at the early stages of this project. J. C. and M. P. C. acknowledge support from the Singapore Ministry of Education through the Academic Research Fund (Tier 2) MOE2017-T2-1-066 (S) and from the NSCC for granting computational resources.

*Corresponding author.
massimo@ntu.edu.sg

- [1] A. Liu and S. Nagel, *Nature (London)* **396**, 21 (1998).
- [2] C. S. O’Hern, S. A. Langer, A. J. Liu, and S. R. Nagel, *Phys. Rev. Lett.* **86**, 111 (2001).
- [3] M. Wyart, *Ann. Phys. Fr.* **30**, 1 (2005).
- [4] L. Berthier and G. Biroli, *Rev. Mod. Phys.* **83**, 587 (2011).
- [5] M. P. Ciamarra, R. Pastore, M. Nicodemi, and A. Coniglio, *Phys. Rev. E* **84**, 041308 (2011).
- [6] M. P. Ciamarra, E. Lippiello, L. de Arcangelis, and C. Godano, *Europhys. Lett.* **95**, 54002 (2011).
- [7] S. Papanikolaou, C. S. O’Hern, and M. D. Shattuck, *Phys. Rev. Lett.* **110**, 198002 (2013).
- [8] D. L. Malandro and D. J. Lacks, *Phys. Rev. Lett.* **81**, 5576 (1998).
- [9] D. L. Malandro and D. J. Lacks, *J. Chem. Phys.* **110**, 4593 (1999).
- [10] C. Maloney and A. Lemaître, *Phys. Rev. Lett.* **93**, 195501 (2004).
- [11] S. Karmakar, E. Lerner, and I. Procaccia, *Phys. Rev. E* **82**, 026105 (2010).
- [12] H. Mizuno, H. Shiba, and A. Ikeda, *Proc. Natl. Acad. Sci. U.S.A.* **114**, E9767 (2017).
- [13] H. G. E. Hentschel, S. Karmakar, E. Lerner, and I. Procaccia, *Phys. Rev. E* **83**, 061101 (2011).
- [14] I. Procaccia, C. Rainone, C. A. B. Z. Shor, and M. Singh, *Phys. Rev. E* **93**, 063003 (2016).
- [15] V. Dailidonis, V. Ilyin, I. Procaccia, and C. A. B. Z. Shor, *Phys. Rev. E* **95**, 031001(R) (2017).
- [16] R. Dasgupta, H. G. E. Hentschel, and I. Procaccia, *Phys. Rev. Lett.* **109**, 255502 (2012).
- [17] R. Dasgupta, H. G. E. Hentschel, and I. Procaccia, *Phys. Rev. E* **87**, 022810 (2013).
- [18] R. Dasgupta, O. Gendelman, P. Mishra, I. Procaccia, and C. A. B. Z. Shor, *Phys. Rev. E* **88**, 032401 (2013).
- [19] R. Mindlin, *Trans. ASME* **16**, 259 (1949).
- [20] See Supplemental Material at <http://link.aps.org/supplemental/10.1103/PhysRevLett.123.098003> for details on the calculation of the Jacobian matrix, and for the demonstration of the robustness of the reported instability to the presence of dissipative forces.
- [21] L. E. Silbert, D. Ertaş, G. S. Grest, T. C. Halsey, D. Levine, and S. J. Plimpton, *Phys. Rev. E* **64**, 051302 (2001).
- [22] H. P. Zhang and H. A. Makse, *Phys. Rev. E* **72**, 011301 (2005).
- [23] S. Plimpton, *J. Comput. Phys.* **117**, 1 (1995).
- [24] J. Chattoraj, O. Gendelman, M. Pica Ciamarra, and I. Procaccia, [arXiv:1901.02376](https://arxiv.org/abs/1901.02376).
- [25] K. Felzer and E. Brodsky, *Nature (London)* **441**, 735 (2006).
- [26] E. E. Brodsky, V. Karakostas, and H. Kanamori, *Geophys. Res. Lett.* **27**, 2741 (2000).
- [27] E. E. Brodsky and N. J. van der Elst, *Annu. Rev. Earth Planet Sci.* **42**, 317 (2014).
- [28] H. Melosh, *Nature (London)* **379**, 601 (1996).
- [29] F. Giacco, L. Saggese, L. de Arcangelis, E. Lippiello, and M. Pica Ciamarra, *Phys. Rev. Lett.* **115**, 128001 (2015).
- [30] D. Mondal, R. Adhikari, and P. Sharma, [arXiv:1904.07783](https://arxiv.org/abs/1904.07783).